Synthesis of Faujasite Zeolites with Crown-ether Templates

Chih-ning Wu and Kuei-jung Chao*
Department of Chemistry, Tsinghua University, Hsinchu, Taiwan, Republic of China

The function of crown ethers in the synthesis of faujasite zeolites has been studied. Hexagonal faujasite (EMT) was prepared from 18-crown-6 ether and not from 15-crown-5 ether as the organic template under hydrothermal conditions, whereas cubic faujasite (FAU) was obtained from a reaction gel using either 18-crown-6 ether or 15-crown-5 ether. During the early stages of synthesis, 18-crown-6 ether and 15-crown-5 ether were partially occluded in the aluminosilicate hydrogel and EMT or FAU nuclei, but 18-crown-6 ether was only adsorbed on the surface of the hydrogel for FAU crystals. Thermal analysis, Raman spectroscopy and composition analysis measurements indicate that sodium cations play a more important role than 18-crown-6 ether in directing the formation of FAU nuclei and balancing the charge on the framework of FAU when 18-crown-6 ether is used at the organic template. The stacking arrangement and Al content of the synthesized faujasite zeolites were found to depend on the SiO_2 : Al_2O_3 and Na_2O : crown ether molar ratios of the reaction mixtures. The structure-directing role of the crown ether in the formation of faujasite zeolites was also studied by theoretical calculations.

Many synthetic studies have been devoted to producing faujasite zeolites with Si : Al < 3 using inorganic bases,[1] and it is possible to obtain a faujasite with Si : Al ≈ 4 using organic templates under hydrothermal conditions.[2,3] Using either tetraethyl orthosilicate or tetramethyl orthosilicate, ZSM-20, an intergrowth of cubic faujasite (FAU) and a hexagonal variant (EMT) was formed.[2,4] FAU and EMT are constructed by the linkage of β-cages through cubic and hexagonal stacking arrangements, respectively.[5] FAU has eight supercages per unit cell that are *ca.* 13 Å in free diameter with four 12-membered ring apertures (7.4 Å) per cage. EMT possesses two types of cage; the first cage (the hypercage)[6] is somewhat elliptical and has a free diameter of *ca.* 14 Å × 13 Å with access *via* five 12-membered ring apertures, the second one (the hypocage)[6] with three 12-membered ring apertures is smaller than either the first type or the supercage of FAU. FAU and EMT were obtained separately in aqueous media using crown ethers. The syntheses of EMT, FAU and the intergrowth of the two forms can be carried out using 18-crown-6 ether, 15-crown-5 ether or a reaction mixture of both templates.[3,7–15] The organic crown ether was found to be very important in directing the stacking arrangement of faujasites.[13–15] In this paper, the function of the crown ether in the syntheses of cubic and hexagonal faujasites is reported. The effect of organic and inorganic bases on the structure and composition of zeolite products were investigated. Raman spectroscopy, thermal analysis, ICP-AES and XRD were used to probe the synthesis process of zeolite. Finally, the synthesis mechanism was proposed and compared with others.[13,15]

Experimental

Synthesis

The reactants were: sodium aluminate [Reidel de Haën, composition (wt%): 54 Al_2O_3 · 41 Na_2O · 5 H_2O], Ludox AS-40 or HS-40 colloidal silica (Du Pont), sodium hydroxide (Merck), 15-crown-5 or 18-crown-6 (Aldrich). The mixture was stirred for 15 min and aged at 20 °C for 24 h, then it was heated in a PTFE-lined stainless-steel autoclave at 115 °C for 7–40 days. At the end of crystallization, the autoclave was quenched to room temperature under tap water. The product was washed thoroughly with deionized water and dried at 70 °C.

Characterization

The crystalline products were identified by X-ray powder diffraction and scanning electron microscopy, using a Rigaku DMAX II diffractometer with Ni-filtered Cu-Kα radiation and a JOEL 840 A electron probe microanalyser. The extent of conversion of EMT and FAU was also estimated by XRD: conversion of EMT (FAU) = [XRD peak area of 2θ = 24.0–24.7° (*ca.* 23.5°) of a solid product]/[XRD peak area of 2θ = 24.0–24.7° (*ca.* 23.5°) of the standard sample]. The crystalline compounds were further examined by thermal analysis and MAS NMR using a Setaram TG/DSC 111 apparatus (with constant heating rate, 10 °C min^{-1}, under an Ar flow) and a Bruker MSL-200 NMR instrument. Typically, more than 3000 free induction decays were accumulated with a π/4 flip angle and 10 s interval for ^{29}Si MAS NMR spectra and more than 500 scans were accumulated with <π/12 of flip angle and 0.5 s interval for ^{27}Al NMR spectra.

Analysis of Reaction Gel

For the preparation of 14 SiO_2 : Al_2O_3 : x Na_2O : 0.7 18-crown-6 ether : 140 H_2O [x = 3.6 (gel A) or 4.8 (gel B) recorded] as well as 10 SiO_2 : Al_2O_3 : 2.4 Na_2O : 0.7 15-crown-5 ether : 140 H_2O (gel C), a set of PTFE-lined autoclaves with identical reactant compositions were heated for various times, quenched and centrifuged. The wet solid phase was directly examined by Raman spectroscopy on a Spectra Physics Ar^+ laser (5145 Å) equipped with a Spex 1401 double-beam spectrometer and an SSR photo-counting system. Typically, the slit width, the scanning rate and the resolution of spectrum were 400 μm, 1.3 s cm^{-1} and 5 cm^{-1}. The composition and pH value of the liquid phase were examined using a GVM 1000 ICP-AES spectrometer and a pH meter. A part of the wet solid was dried at ambient temperature for 3 days, then examined by XRD and TG/DSC.

Computer Modelling

All calculations were performed with Cerius2 software (MSI). The applied force field is burchart 1.01-DREIDING 2.11, which is especially useful for the study of properties of organic molecules inside zeolite frameworks. The structures of EMT and FAU used the data of Baerlocher *et al.*[16] and Mortier *et al.*[17] with an Si : Al ratio of 3.3, to be consistent with Loewenstein's law. The unit-cell formulae of EMT and FAU are ($Na^{\cdot+}$ crown-ether) $Na_{43}(SiO_2)_{148}(AlO_2)_{44}\cdot 6H_2O$ and ($Na^{\cdot+}$ crown-ether) $Na_{21}(SiO_2)_{74}(AlO_2)_{22}\cdot 16H_2O$,

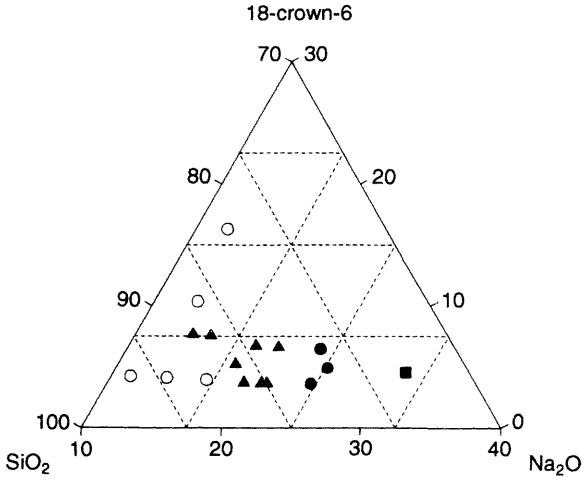

Fig. 1 Approximate crystallization field of zeolites in the SiO_2–Na_2O–(18-crown-6) systems at 115 °C (with starting $SiO_2 : Al_2O_3 = 10$ or 14 and mol% SiO_2 + mol% 18-crown-6 + mol% Na_2O = 100%). ▲, EMT; ■, GIS; ●, FAU; ○, amorphous products.

respectively. The local charges on each atom of Na^{*+} crown ether were estimated by the QEq method with C, O and Na^+ partial charges of 0.05, −0.51 and +1, respectively, and a total charge of +1; while the partial charges of the zeolite framework Si, Al, O and extra framework hydrated Na^+ ion, O of H_2O are correspondingly assigned to 0.29, 0.46, −0.27 and 0.91, −0.08, the total charge of being −1. The whole system of Na^{*+} crown ether/zeolite is neutral. The structures of EMT and FAU were relaxed to their minimum-energy

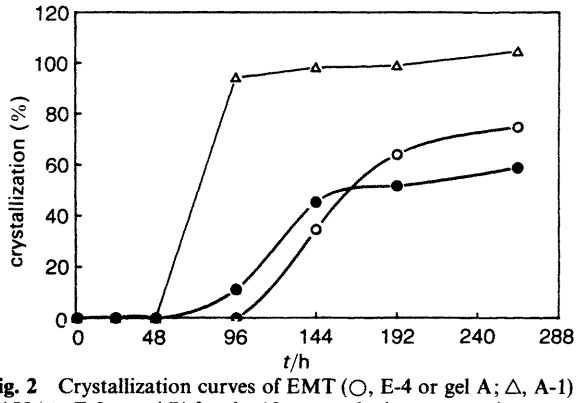

Fig. 2 Crystallization curves of EMT (○, E-4 or gel A; △, A-1) and FAU (●, E-8 or gel B) for the 18-crown-6 ether preparations

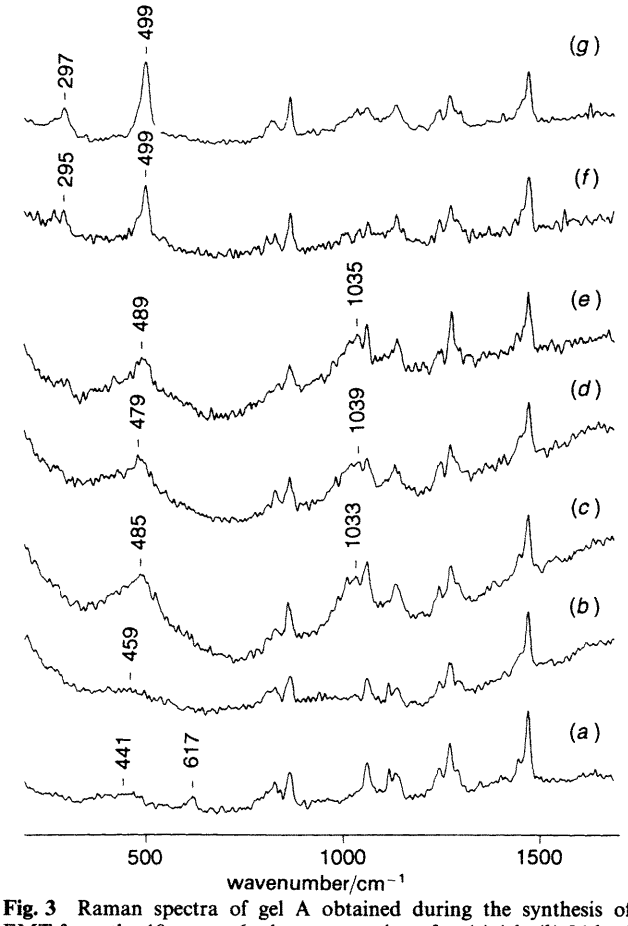

Fig. 3 Raman spectra of gel A obtained during the synthesis of EMT from the 18-crown-6 ether preparation after (*a*) 1 h, (*b*) 24 h of aging at room temperature and (*c*) 1 day, (*d*) 3 days, (e) 5 days, (*f*) 7 days and (*g*) 10 days of heating at 115 °C

conformations under constant pressure first, then the optimized locations and host–guest interactions of crown ethers in large cages were probed by molecular dynamics and energy minimization. During simulation, the conformations of one or two crown ethers in the unit cell of (111) or (221) are varied while the frameworks are kept fixed. Finally, the morphological simulations were carried out using the 'attachment energy' method of Cerius2, which relies on a calculation of the energy released when a growth slice is added to a growing plane.

Table 1 Dependence of the formation of zeolite on the reactant composition

composition of initial mixtures							product		
								Si : Al[b]	
sample	SiO_2	Al_2O_3	Na_2O	18-C-6[a]	15-C-5[a]	t/days	phase	^{29}Si NMR	ICP-AES
A-1	10	1	2.4	0.7		7	EMT	3.30	3.38
A-2	10	1	2.0	1.0		10	EMT	3.88	3.92
A-4	10	1	1.8	1.0		40	EMT	4.00	
C-1	10	1	3.6	0.7		7	FAU	2.61	2.36
C-2	10	1	4.8	0.7		7	GIS	2.06	1.68
E-4	14	1	3.6	0.7		7	EMT	3.92	3.75
E-5	14	1	3.9	0.7		7	EMT/FAU	3.79	3.58
E-8	14	1	4.8	0.7		7	FAU	2.91	2.74
H-2	10	1	2.4		0.7	7	FAU	3.60	
I-3	14	1	4.8		0.7	7	FAU	2.72	

[a] 18-C-6 = 18-crown-6 ether and 15-C-5 = 15-crown-5 ether. [b] The values were determined by ^{29}Si MAS NMR and ICP-AES.

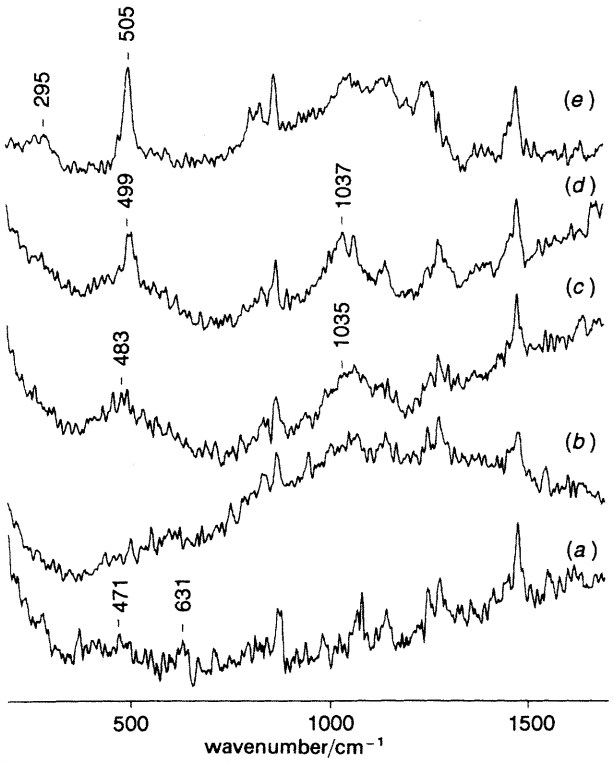

Fig. 4 Raman spectra of gel B obtained during the synthesis of FAU from the 18-crown-6 ether preparation after (*a*) 1 h, (*b*) 24 h of aging at room temperature and (*c*) 1 day, (*d*) 3 days and (*e*) 5 days of heating at 115 °C

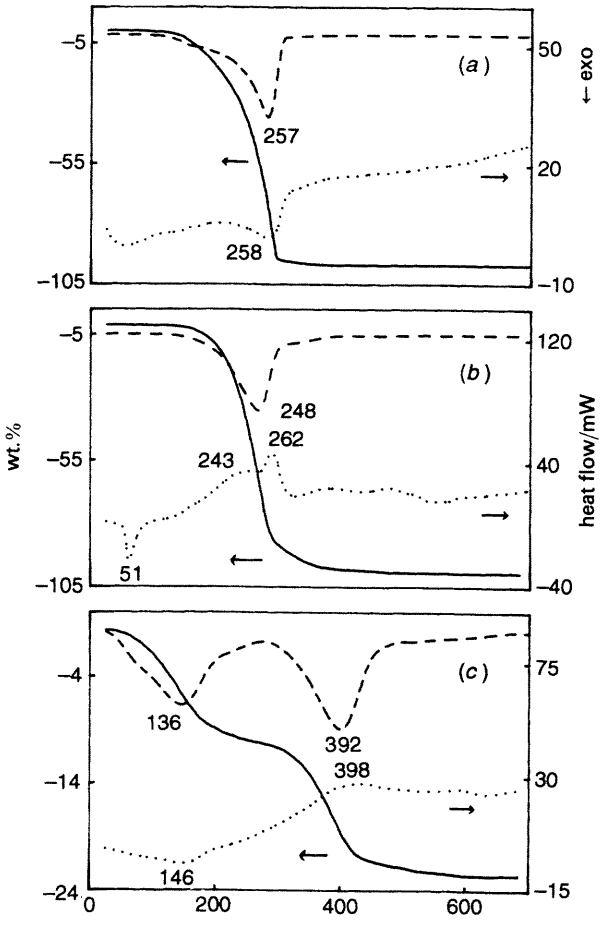

Fig. 5 TG (——), DSC (· · ·) and DTG (– – –) curves of (*a*) 15-crown-5 (liquid), (*b*) 18-crown-6 (solid), (*c*) 18-crown-6 · EMT (E4)

Results

EMT formed from 18-crown-6 but not from 15-crown-5 templates, whereas FAU was obtained from a gel with either 18-crown-6 ether or 15-crown-5 ether.[18] Similar results were observed by Burkett and Davis[13] and Feijen *et al.*[15] EMT, FAU and GIS zeolites crystallized sequentially from reactant gels with $SiO_2 : Al_2O_3$ molar ratios of 10 or 14 and increasing Na_2O : 18-crown-6 ratios as shown in Fig. 1. By controlling the Na_2O : 18-crown-6 ratio, an intergrowth of EMT and FAU was also obtained (*e.g.* E-5, in Table 1). Moreover, a higher molar ratio of $SiO_2 : Al_2O_3$ in the starting composition led to a lower crystallization rate to form EMT when using a similar $Na_2O : SiO_2$ ratio (Fig. 2, *cf.* A-1 and E-4). Increasing the molar ratio of Na_2O : 18-crown-6 caused rapid dissolution of reactant silica and exhaustion of aluminate ions; in turn, the rate of zeolite formation could be accelerated, but the form of zeolite produced might by FAU instead of EMT (Fig. 2, *cf.* E-4 and E-8). Based on the above results, the $SiO_2 : Al_2O_3$ ratio of the reactant mixture is a major factor in the control of the crystallization rate. However, the Si : Al ratios of both EMT and FAU decrease with increasing Na_2O : crown-ether ratio in the reaction mixture with constant $SiO_2 : Al_2O_3$ ratio and crown ether concentration as shown in Table 1.

Raman Spectroscopy and XRD

Fig. 3 and 4 show the room-temperature Raman spectra of the gel phase obtained during aging at ambient temperature and reaction at 115 °C. In the early stages of aging, insoluble silica from Ludox AS-40 and unreacted $Al(OH)_4^-$ retained in the gel A gives bands at *ca.* 441 and *ca.* 617 cm^{-1},[19] respectively. At the end of aging, the $Al(OH)_4^-$ species in the solid part and Al species in the solution part of gel A are found almost to disappear, as determined by Raman spectroscopy and ICP-AES; this may result from the formation of the aluminosilicate hydrogel, which is considered to be the precursor of zeolite. The solid SiO_2 spheres may be surrounded by an $Al(OH)_n$ sheath to give a broad band around 459 cm^{-1}. Upon heating, the insoluble silica dissolves progressively so that the concentration of silicates in solution measured by ICP-AES increases significantly. After the sample has been heated for 1–5 days the cyclic tetrameric aluminosilicate and silicate anions are observed at 479–489 cm^{-1} (the T–O–T bending of tetrameric species, T = Si or Al) and at 1033–1039 cm^{-1} (the Si—O stretching mode).[20] The powder X-ray data (Fig. 2) indicate that the crystalline phase can be detected after either 3 or 5 days of heating. The formation of EMT gives two characteristic bands at 295–297 and 499 cm^{-1} that correspond to a low-frequency torsion mode from the cation–lattice interaction and a T–O–T vibration of the four-membered aluminosilicate rings of the zeolite.[19] The bands in the range 700–1700 and 2700–3100 cm^{-1} (unshown) are characteristic of the crown ether. There is a slight difference in intensity and splitting pattern between Na^{+} crown-ether complex molecules in solution and in the zeolite, indicating that the perturbation of the complex by the EMT framework is minimal.

As shown in Table 1, the 18-crown-6 gel with low and high Na_2O contents yielded EMT and FAU, respectively. The Raman spectra of the solid part of gel B are similar to those of gel A, as shown in Fig. 4. During aging, the aluminate (*ca.* 631 cm^{-1}) is adsorbed on the surface of the silica (*ca.* 471 cm^{-1}). The tetrameric silicate or aluminosilicate (*ca.* 483 and *ca.* 1035 cm^{-1}) is present after 1 day of heating. Finally, the FAU crystals formed give two bands: the 4-ring T–O–T bending near 505 cm^{-1} and the cation–lattice torsion mode at *ca.* 295 cm^{-1} (after 5 days of heating).

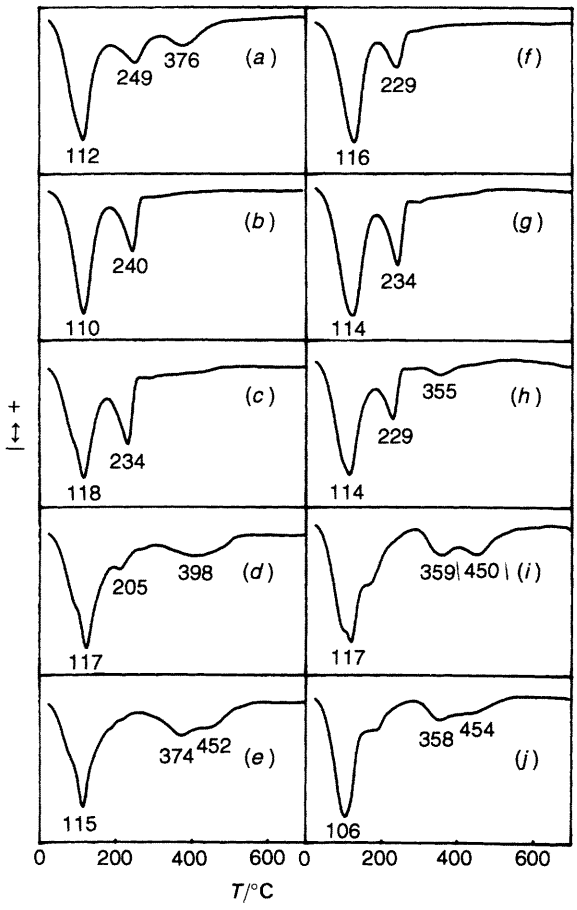

Fig. 6 DTG curves of gel A after (*a*) 24 h of aging at room temperature and (*b*) 1 day, (*c*) 3 days, (*d*) 5 days and (*e*) 7 days of heating at 115 °C, and gel B after (*f*) 24 h of aging at room temperature and (*g*) 1 day, (*h*) 3 days, (*i*) 5 days and (*j*) 7 days of heating at 115 °C

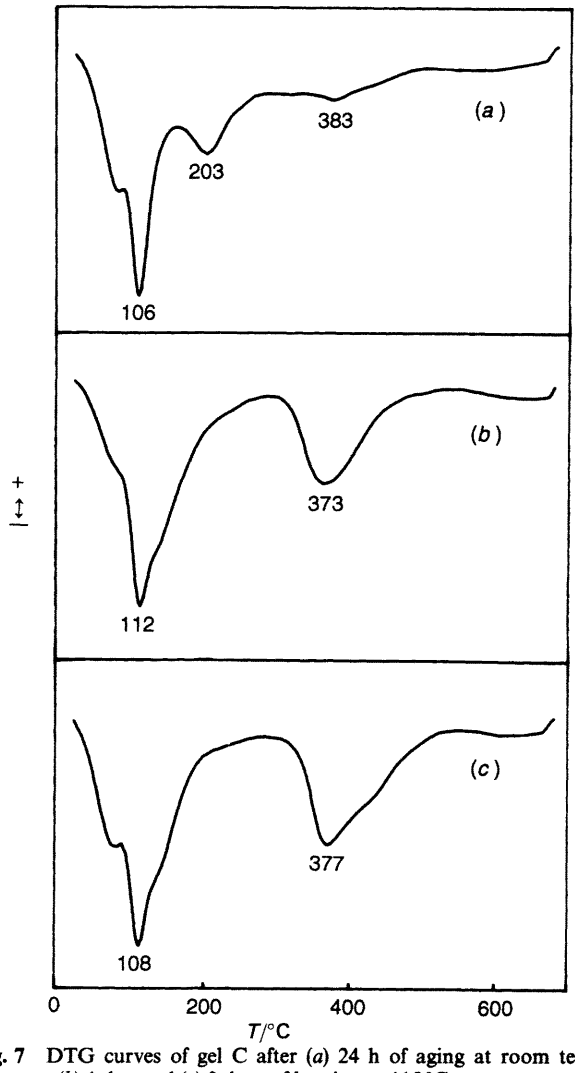

Fig. 7 DTG curves of gel C after (*a*) 24 h of aging at room temperature, (*b*) 1 day and (*c*) 3 days of heating at 115 °C

Although the symmetries of FAU and EMT are different, with space groups of Fd^3m (O_h^7) and $P6_3/mmc$ (D_{6h}^4), respectively, the frequency of the strongest band corresponding to T–O bending vibrations of four-membered rings in EMT (at *ca.* 499 cm^{-1}) is similar to that in FAU (at *ca.* 505 cm^{-1}). Both EMT and FAU contain 4-, 6- and 12-membered rings. The 4-ring building units can be investigated by Raman spectroscopy, but 6- and 12-rings cannot. The linkage of the 4-rings to other 4-rings and 6-rings in the gel changes from a random (amorphous) to an ordered form (crystal phase), and the corresponding 4-ring band consequently becomes sharper. The XRD measurements also show that the rate of nucleation of FAU from gel B is faster than that of EMT from gel A (Fig. 2). By Raman spectroscopy, the differences between the structures of EMT and FAU could not be distinguished exactly and the role played by the Na^{*+} crown-ether complex during crystallization remained uncertain. However, the formation of a hydrogel precursor and the 4-ring building unit and the process of crystal growth could be probed by this technique.

Thermal Analysis

The TG/DSC thermal analysis with on-line mass spectrometry showed three distinct stages of weight loss on the faujasites: 25–200 °C, 200–300 °C and 300–500 °C. The first endotherm is mainly due to the desorption of water, while the second and third result from the exothermic decomposition of crown ether in faujasite zeolites [Fig. 5(*c*)]. The decomposition of bulk 15-crown-5 and 18-crown-6 ethers occurs in the range 150–300 °C [Fig. 5(*a*) and (*b*)]. TG and DSC data were obtained using the same instrument, and the DTG curve was obtained from the TG curve by manual differentiation, *i.e.* the derivative of the mass-change with respect to temperature. Because the response to heat transfer by the calorimetric fluxmeter in DSC is slower than the response to mass change by the thermobalance in TG/DTG, the values of T_{max} (the temperature at which mass loss is the most rapid in DTG) are usually smaller than those of T_{top} (the maximum temperature of a peak in DSC). Fig. 6 shows the DTG data of the gel during the zeolite crystallization process. For gel A to produce EMT as the end-product [Fig. 6(*a*)], the 18-crown-6 ether was found to be either adsorbed on the surface of the amorphous gel (T_{max} = 249 °C) or enclosed in the aluminosilicate hydrogel (T_{max} = 376 °C), which is the precursor to EMT, after 24 h of aging. When the sample was heated for 1–3 days, the aluminosilicate hydrogel progressively dissolved. Thus, the third peak shown in the DTG was reduced. After 5 days of heating, EMT was formed; part of the ether was intercalated into the hypercages or hypocages of EMT (T_{max} = 398 °C), instead of being adsorbed on the surface of the amorphous gel. At the end of the reaction (7 or 10 days of heating), T_{max} at 374 °C and 452 °C on the DTG might correspond to two types of intercalation of crown ethers in EMT [Fig. 6(*e*)].

For gel B, the DTG spectrum in Fig. 6(*f*) shows one type of 18-crown-6 ether (T_{max} = 229 °C) upon aging (1–24 h). This indicates that crown ethers may only be adsorbed on the

surface of the amorphous gel and not occluded in the precursor hydrogel in the nucleation period of FAU. Fig. 6(*h*)–(*j*) show that the 18-crown-6 ether can be entrapped in FAU crystals in the final stage of synthesis with a decomposition temperature of T_{max} = *ca.* 360 or 450 °C. 15-Crown-5 ether is also enclosed in the aluminosilicate hydrogel (T_{max} = 383 °C) precursor of FAU, during aging for 24 h in gel C (Fig. 7). Owing to the faster crystal growth, the crown ether is encapsulated into the supercages of FAU after either 1 or 3 days of heating.

ICP-AES

The concentrations of aluminate, silicate and sodium species in solutions were analysed by ICP-AES. For both gels A and B, the Si contents (*ca.* 0.02 mol l^{-1}) in solutions were negligible as long as an appreciable level of soluble Al species (0.5–0.6 mol l^{-1}) was present. This may result from the adsorption of $Al(OH)_4^-$ ions on the silica surface that can prevent the silica from dissolving.[21] The concentration of soluble aluminate species was reduced when aluminosilicate hydrogels were formed upon aging and heating the sample at 115 °C; the concentration of silicates (2.1–2.3 mol l^{-1}) in solution was increased by the depletion of Al (0.02–0.04 mol l^{-1}) from solution. The concentration of dissolved silicate species emanating from hydrogels was much higher than that emanating from reactant mixtures.

The loss of silicates from solution to zeolite crystals may be compensated by dissolution of the solid phase of the gel so that the concentration of Si in solution of both gels remains almost constant during heating. Moreover, there are slight changes in the average molar ratios of Na : Al and Al : Si in solution during the crystal growth of zeolites. It seems that a quasi-equilibrium exists between the solid and solution phases of the aluminosilicate gel, as suggested by Zhdanov.[22] The pHs of the solutions were kept at 11.5 (gel A) or *ca.* 12.0 (gel B) after 1 day of heating.

Discussion

The ICP-AES measurements indicate that the zeolite nuclei, the hydrogel precursor and the liquid solution are in equilibrium during crystallization. Because of the existence of this equilibrium, the specific precursor or hydrogel can play a very important role in influencing the form of nuclei and final products. As shown by thermal analysis, the encapsulation of organic templates or inorganic cations in the hydrogel seems to determine the type of zeolite product. Moreover, the concentrations of aluminate ion, silicate ion and NaOH in aqueous solution significantly affect the crystal growth rate and the composition of the zeolite crystals. According to the above results, a mechanism is proposed in Fig. 8. The aluminate and silicate or polysilicate anions in solution can form a hydrogel; a strong base such as NaOH accelerates the dissolution of the gel materials and the formation of $Al(OH)_n$; the soluble silicate and aluminate ions may regroup around the hydrated inorganic (sodium) cations or organic templates ($Na^{\bullet+}$ 18-crown-6 or $Na^{\bullet+}$ 15-crown-5 complexes) to form the nuclei of FAU or EMT zeolite. However, compared with the $Na^{\bullet+}$ crown ether complex, the hydrated Na^+ cation in the hydrogel (or precursor) seem to attract aluminosilicate species more than the silicate species. As shown in Fig. 8, the hydrated sodium cations can offset the charges of alumina tetrahedra and direct the formation of the aluminosilicate hydrogel for FAU nuclei, and then the $Na^{\bullet+}$ 18-crown-6 ether complex may involve the process of crystal growth and increase the Si : Al ratio of FAU crystals to *ca.* 2.9 (higher than the Si : Al ratio of 2.4 from the conventional inorganic

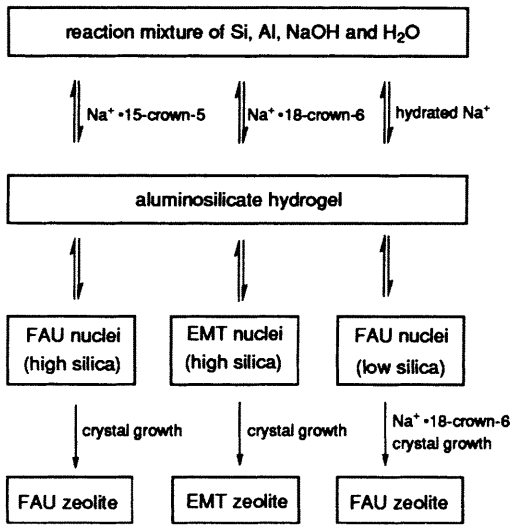

Fig. 8 Synthetic scheme of zeolites EMT and FAU in the 18-crown-6 or 15-crown-5 ether preparation

base preparation). The $Na^{\bullet+}$ 18-crown-6 and $Na^{\bullet+}$ 15-crown-5 mediated syntheses result in higher Si : Al ratios of EMT (3.8) and FAU (3.3), respectively.

The structure-directing role of the crown ether in the synthesis of EMT and FAU was also approached by theoretical calculations. Combining the methods of molecular dynamics and energy minimization, the optimized locations and stabilization energies of $Na^{\bullet+}$ crown ether complexes within various large cages of EMT and FAU were estimated. In this study, both one crown ether in one cage and two crown ethers in two neighbouring cages gave the same trend for stabilization energies, as shown in Table 2. It is useful to compare this observation with the effect of a tetraalkylammonium ion in the MFI cage on a neighbouring organic template ion.[23] The optimum locations (those with the lowest energy) of the $Na^{\bullet+}$ crown ether complex encapsulated in the supercage of FAU and the hypercage or hypocage of EMT are found to face perpendicular to the 6-membered ring of the sodalite cage in FAU and to orient perpendicular to the *c*-axis of EMT crystal, respectively. The optimum location of $Na^{\bullet+}$ 18-crown-6 in EMT is consistent with the X-ray diffraction result of Baerlocher *et al.*[16] The calculated results in Table 2 also indicate that the $Na^{\bullet+}$ 18-crown-6 complex is more stable in the hypocage of EMT (with a stabilization energy of 37–40 kcal mol^{-1}) than in the supercage of FAU (29 kcal mol^{-1}) or the hypercage of EMT (28 kcal mol^{-1}). The $Na^{\bullet+}$ 18-crown-6 complex seems to be a more favourable template for forming EMT than FAU. This is consistent with the result of Feijan *et al.*,[15] who suggest that the hydrated sodium cations determine the formation of 'faujasite sheets', while the $Na^{\bullet+}$ 18-crown-6 complex is responsible for the linkage of these sheets with hexagonal (in the sequence ABAB) instead of cubic symmetry (ABCABC sequence). Our calculated results indicate that the $Na^{\bullet+}$ 18-crown-6 complex can strongly stabilize the faujasite layer (*i.e.* the *ab* planes of EMT) *via* tight fitting and interact with the wall of hypocage of EMT. The $Na^{\bullet+}$ 18-crown-6 complex may also affect the mode of stacking of the neighbouring layers to link, in the direction of the *c* axis and with mirror-image symmetry, by stabilizing the hypercage. Therefore, Burkett *et al.* found that the presence of the $Na^{\bullet+}$ 18-crown-6 complex in the hypocage is important in the synthesis of EMT.[13] However, the stabilizing effect of the crown ether in the hypocage and hypercage can play an essential role in the stacking of the faujasite sheets to form EMT topology, as shown by the simulation (Fig. 9).

Table 2 Host–guest interactions between crown ethers and faujasite-type zeolites

template/zeolite	host–guest interaction/kcal mol^{-1} [a]	
	one template in one cage	two templates in adjoining cages
(*a*) lattice of (*abc*) = (221):[b]		
$Na^{\bullet+}$ 18-crown-6/EMT (hypocage)	−40	−49[c]
$Na^{\bullet+}$ 18-crown-6/EMT (hypercage)	−28	−35
$Na^{\bullet+}$ 15-crown-5/EMT (hypocage)	−34	—
$Na^{\bullet+}$ 15-crown-5/EMT (hypercage)	−21	—
(*b*) lattice of (*abc*) = (111):		
$Na^{\bullet+}$ 18-crown-6/EMT (hypocage)	−37	−57
$Na^{\bullet+}$ 18-crown-6/FAU (supercage)	−29	−44
$Na^{\bullet+}$ 15-crown-5/EMT (hypocage)	−29	—
$Na^{\bullet+}$ 15-crown-5/FAU (supercage)	−24	−39

[a] The host–guest interaction is estimated as: (total energy of template/zeolite) − (lattice energy of zeolite) − (energy of template). [b] (221) represents a lattice of $2a \times 2b \times c$, where a, b, c are the cell dimensions. [c] Eight templates are located in eight hypocages of the (221) unit cell.

The difference in stabilization energies of $Na^{\bullet+}$ 18-crown-6 in the hypocage and hypercage of EMT may influence the crystal growth rates along the ***a***, ***b*** and ***c*** axes and result in a faster rate in the direction of the *ab* plane than along the ***c*** axis; in turn, the hexagonal morphology of EMT with a short ***c*** axis (observed by SEM) is generated. This agrees well with the investigation of high-resolution electron microscopy by Terasaki *et al.*,[14] who observed that the growth of EMT with 18-crown-6 ether is strongly anisotropic, *i.e.* the growth rate in the 001_{HEX} planes is *ca.* 15 times faster than that in the 100_{HEX} and 010_{HEX} planes. The simulation of the morphology showed that the $Na^{\bullet+}$ 18-crown-6 complex being occluded in a more stable manner in the hypocage than the hypercage is the major factor in generating the specific hexagonal morphology of EMT (as shown in Fig. 9).

The $Na^{\bullet+}$ 15-crown-5 complex hypothetically occluded in either the hypocage (29–34 kcal mol^{-1}) or hypercage (21 kcal mol^{-1}) of EMT may not improve the stability of the faujasite layers in forming the EMT topology, in contrast to the case of the $Na^{\bullet+}$ 18-crown-6 complex. With respect to the synthesis of FAU in the presence of 15-crown-5 ether, the host–guest energy of 24 kcal mol^{-1} indicates that the $Na^{\bullet+}$ 15-crown-5 complex may stabilize the supercage of FAU only weakly. It is likely that the excess of hydrated Na^+ cations plays a more important role than the $Na^{\bullet+}$ 15-crown-5 complex in directing the structure of FAU. Burkett and Davis[13] and Terasaki *et al.*[14] reached a similar conclusion. They suggested that the structure-directing role of 15-crown-5 in the formation of FAU was not clearly verified and is still under debate. However, the $Na^{\bullet+}$ 15-crown-5 complex was encapsulated in the hydrogel precursor, as shown by our thermal analysis data, and might facilitate the enhancement of the Si : Al ratio of FAU by more than 3. Furthermore, the results of the simulation indicate that the presence of the $Na^{\bullet+}$ 18-crown-6 complex or the $Na^{\bullet+}$ 15-crown-5 complex within the supercage cannot influence the cubic morphology of FAU and the cubic symmetry can also be generated in the presence of hydrated sodium cations.

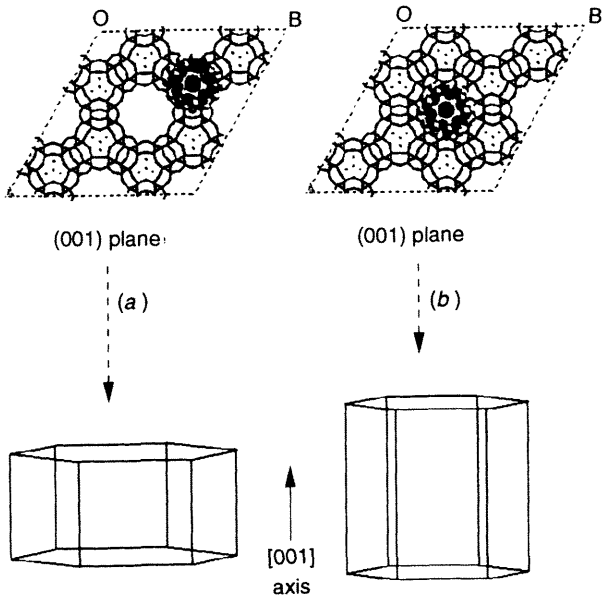

Fig. 9 Simulated morphologies derived from NaEMT containing one $Na^{\bullet+}$ 18-crown-6 complex in the (*a*) hypocage and (*b*) hypercage (solid dots represent Na^+ ions)

Conclusions

The variations of $SiO_2 : Al_2O_3$ and crown ether : Na_2O ratios in the reactant mixture not only influence the rate of zeolite nucleation and crystallization, but also affect the formation of precursor aluminosilicate gel and the stacking arrangement of the zeolite.

The authors thank the National Science Council, ROC for financial support, the National Center for High-Performance Computing, Taiwan, for the provision of MSI technology and Professor Hua Chang for the Raman instrument and helpful discussions.

References

1 D. W. Breck, in *Zeolite Molecular Sieves*, Wiley, New York, 1974, ch. 4.
2 S. Ernst, G. T. Kokotailo and J. Weitkamp, *Stud. Surf. Sci. Catal.*, 1988, **37**, 29.
3 F. Delprato, L. Delmotte, J. L. Guth and L. Huve, *Zeolites*, 1990, **10**, 546.
4 J. M. Newsam, M. M. J. Treacy, D. E. W. Vaughan, K. G. Strohmaier and W. J. Mortier, *J. Chem. Soc., Chem. Commun.*, 1989, 493.
5 J. L. Lievens, J. P. Verduijn, A. J. Bons and W. J. Mortier, *Zeolites*, 1992, **12**, 698.
6 J. A. Martens, P. A. Jacobs and S. Cartlidge, *Zeolites*, 1989, **9**, 423.

7 J. Dwyer, K. Karim, W. J. Smith, N. E. Thompson, R. K. Harris and D. C. Apperley, *J. Phys. Chem.*, 1991, **95**, 8826.
8 J. P. Arhancet and M. E. Davis, *Chem. Mater.*, 1991, **3**, 567.
9 M. J. Annen, D. Young, J. P. Arhancet, M. E. Davis and S. E. Schramm, *Zeolites*, 1991, **11**, 98.
10 M. W. Anderson, K. S. Pachis, F. Prébin, S. W. Carr, O. Terasaki, T. Ohsuna and V. Alfreddson, *J. Chem. Soc., Chem. Commun.*, 1991, 1660.
11 F. Dougnier, J. Patarin, J. L. Guth and D. Anglerot, *Zeolites*, 1992, **12**, 160.
12 G. W. Skeels, C. S. Blackwell, K. B. Reuter, N. K. McGuire and C. A. Bateman, in *Proceedings of the 9th International Zeolite Conference*, Butterworth–Heinemann, Montreal, 1993, p. 415.
13 S. L. Burkett and M. E. Davis, *Microporous Mater.*, 1993, **1**, 265.
14 O. Terasaki, T. Ohsuna, V. Alfredsson, J. O. Bovin, D. Watanabe, S. W. Carr and M. W. Anderson, *Chem. Mater.*, 1993, **5**, 452.
15 E. J. P. Feijen, K. De Vadder, M. H. Bosschaerts, J. L. Lievens, J. A. Martens, P. J. Grobet and P. A. Jacobs, *J. Am. Chem. Soc.*, 1994, **116**, 2950.
16 C. Baerlocher, L. B. McCusker and R. Chiappetta, *Microporous Mater*, 1994, **2**, 269.
17 W. J. Mortier, E. Van den Bossche and J. B. Uytterhoeven, *Zeolites*, 1984, **4**, 41.
18 C. N. Wu, Masters Thesis, Tsinghua University, Taiwan, 1993.
19 J. Twu, P. K. Dutta and C. T. Kresge, *J. Phys. Chem.*, 1991, **95**, 5267; *Zeolites*, 1991, **11**, 672.
20 P. K. Dutta and D. C. Shieh, *Appl. Spectrosc.*, 1985, **39**, 343.
21 R. K. Iler, *J. Colloid Interface Sci.*, 1973, **43**, 399; *The Colloidal Chemistry of Silica and Silicates*, Ithaca, New York, 1955, p. 18.
22 S. P. Zhdanov, *Adv. Chem. Ser.*, 1971, **101**, 20.
23 R. G. Bell, D. W. Lewis, P. Voigt, C. M. Freeman, J. M. Thomas and C. R. A. Catlow, in *Studies in Surface Science and Catalysis*, ed. J. Weitkamp, H. G. Karge, H. Pfeifer and W. Hölderich, Elsevier, Garmisch-Partenkirchen, Germany, 1994, p. 2075.

Paper 4/03668I; *Received* 17*th June*, 1994